Theory meets experiment for elucidating the structure and stability of non-covalent complexes: Water-Amine interaction as a proof of concept

ARTICLE

Theory Meets Experiment for Elucidating the Structure and Stability of Non-covalent Complexes: Water-Amine Interaction as a Proof of Concept

Received 00th January 20xx,
Accepted 00th January 20xx

DOI: 10.1039/x0xx00000x

Junhua Chen,[†a] Yang Zheng,[†a] Alessio Melli,[†b] Lorenzo Spada,[bc] Tao Lu,[a] Gang Feng,[ad] Qian Gou,[*ad] Vincenzo Barone,[*c] and Cristina Puzzarini[*b]

Severa gas phase spectroscop c nvest gat ons have focused on a better understand ng of the nature of weak, non cova ent nteract ons n mode systems. However, the r character zat on and nterpretat on are st far from be ng sat sfactory. A prom s ng route to f th s gap s offered by strateg es n wh ch h gh reso ut on rotat ona spectroscopy s deep y ntegrated w th state of the art quantum chem ca methodo ogy to accurate y determ ne ntermo ecu ar parameters and nteract on energ es, w th the atter nterpreted by means of powerfu energy decompos t on ana yses (EDAs). As a proof of concept of th s approach, we have se ected the adducts formed by n propy am ne (PA) and so propy am ne (IPA) w th water. Among the stab e structures computat ona y pred cted, four (out of f ve) somers of the PA water comp ex and two somers (*trans* and *gauche*) of the IPA water adduct have been character zed w th superson c jet Four er transform m crowave spectroscopy. Start ng from the exper menta rotat ona constants for d fferent sotop c spec es, computat on of the correspond ng v brat ona correct ons a owed a sem exper menta determ nat on of the ntermo ecu ar parameters. D fferent EDAs po nt out that n a cases a strong O H···N hydrogen bond s the pr mary nteract on. Accurate computat ons nd cate that the ength and ram f cat on of the a ky cha n do not s gn f cant y affect the water am ne nteract ons, wh ch on the contrary mod fy the stab ty order of so ated PA conformers.

Introduction

Non-covalent molecular complexes, in addition to their intrinsic interest, provide the unique opportunity to gain insights on the interactions of a given molecule with the environment and, in particular, in condensed phases. Indeed, the first step toward their understanding is a complete characterization of the basic interactions occurring between one target molecule and one "environmental" species, with water being that of greatest interest. As a matter of fact, gas-phase investigations of non-covalent molecular complexes provide structural and dynamical information that is seldom straightforward to be derived from measurements in condensed phases. To exploit such investigations at best, a powerful strategy relies on high-resolution rotational spectroscopy supported and complemented by state-of-the-art quantum-chemical (QC) computations (see, e.g., refs. 1-4). Although a large number of spectroscopic studies of molecular complexes also reporting some QC calculations can be found in the literature (see, e.g., refs. 1,5-9), there is still a lack of full integration between experiment and theory, thus preventing a full reconciliation of accuracy and interpretation. Illustrative in this respect is the fact that the usual practice for deriving structural information from rotational spectra of different isotopic species is to rely on questionable, "old-fashioned" approximations such as the so-called substitution structure. On the other hand, the semi-experimental approach,[10] well-tested for isolated molecules (see, e.g., refs. 11-14), allows the determination of not only equilibrium intramolecular, but also intermolecular, parameters with great accuracy (0.001 Å for distances and 0.1 degrees for angles) by combining experimental rotational constants with computed vibrational corrections. A further aspect of this strong interplay of experiment and theory is the derivation of interaction energies with uncertainties as low as a fraction of kJ mol^{-1} combined with their interpretation in terms of chemically meaningful concepts by means of energy decomposition analyses (EDAs).

As a proof of concept of this approach, we have chosen the interaction between the primary amino group (-NH_2) and water, which plays a key role in several fields ranging from biology to atmospheric chemistry and astrochemistry. Despite the fact that several spectroscopic studies of water adducts with ammonia and amines have been previously reported, the number of investigations involving primary amines is quite limited (see, e.g., refs. 15-20). Hydrogen bonds (HBs) are ubiquitous in organic or biological molecules involving either oxygen or nitrogen, their topologies and strengths being significantly tuned by the functional groups bonded to the

[a] *Department of Chemistry, School of Chemistry and Chemical Engineering, Chongqing University, Daxuecheng South Rd. 55, 401331 Chongqing, China.*
[b] *Department of Chemistry "Giacomo Ciamician", University of Bologna, Via F. Selmi 2, 40126 Bologna, Italy.*
[c] *Scuola Normale Superiore, Piazza dei Cavalieri 7, 56126 Pisa, Italy.*
[d] *Chongqing Key Laboratory of Theoretical and Computational Chemistry, Chongqing University, Daxuecheng South Rd. 55, 401331 Chongqing, China.*
[†] *These authors contributed equally to this work.*
Electronic Supplementary Information (ESI) available: PDF file collecting all transitions recorded together with the corresponding spectroscopic parameters from the fit. Detailed results from the SAPT and NBO analyses are also reported. See DOI: 10.1039/x0xx00000x

interacting atoms. In this respect, the tuning of amine-water interaction by the length and/or ramification of the alkyl chain has not been fully characterized yet and any generalization from small to large alkyl amines is completely missing.

Alkyl amines have been detected systematically in the atmosphere[21-25] and represent one important class of compounds involved in the complex organic fraction of ambient aerosol and play a pivotal role in aerosol growth processes (see, e.g., refs. 21-23) and in determining the hygroscopic properties of particles.[24] Although intermolecular complexes are not of direct astrophysical interest, ices, hydrates, and clathrates are formed from ammonia and other amines. The coexistence of a number of hydrate-clathrate systems[26,27] might determine, in part, the volatile inventories of comets, icy satellites, and other objects.[28,29] Last but not least, the fine tuning of amine properties has significant implications for their increasing employment in nano-engineering.[30,31] These examples point out that a deeper understanding of how amines interact with water warrants a thorough investigation. As a matter of fact, the development of amine-water intermolecular parameters is an area of active development,[32,33] which –however– suffers from the lack of accurate structures and interaction energies for reference amine-water complexes.

The above considerations prompted us to undertake a comprehensive study of the molecular complexes formed by n-propylamine (PA) and iso-propylamine (IPA) with one water molecule (W) by means of an integrated computational-experimental approach, which has already provided remarkable results in some recent studies.[3,4,34] PA and IPA have been selected because they represent a good compromise: on the one hand, they are systems with an alkyl chain sufficiently long to lead to significant effects; on the other hand, the sizes of their water complexes are such that they are still amenable to high-level QC calculations. To complement such investigation, the molecular complexes involving smaller primary amines, namely methylamine (MA) and ethylamine (both *trans*, ET, and *gauche*, EG), with one water molecule have also been characterized from a computational point of view in order to unveil general trends related to the lengthening of the alkyl chain.

Computational Methods

The conformational potential energy surfaces (PESs) of both the PA-W and IPA-W adducts have been investigated using the B2PLYP-D3(BJ) double-hybrid functional[35] (with D3(BJ) denoting the correction for dispersion effects according to the Grimme's DFT-D3[36] scheme employing the Becke-Johnson damping function[37]) in conjunction with the maug-cc-pVTZ-*d*H basis set,[38] where "-*d*H" denotes that *d* functions on hydrogen atoms have been removed.[39] Geometry optimizations have been performed by both including and neglecting the counterpoise correction (CP)[40] to recover the basis set superposition error (BSSE), thus leading to two levels of theory shortly denoted as B2-CP and B2, respectively. While CP corrections are mandatory in order to obtain reliable and accurate interaction energies, their inclusion in geometry optimizations might lead to a potential improvement of the results, as recently demonstrated in ref. 41.

All stationary points have been confirmed and characterized by evaluating the corresponding Hessian matrix (harmonic force field in a normal mode representation) at the B2 level by means of analytical second derivatives.[42] Subsequently, energetics has been improved using the so-called "cheap" composite scheme (hereafter, simply referred to as ChS).[43-45] In this approach, the energy obtained using the coupled-cluster singles and doubles approach with perturbative inclusion of triple excitations, CCSD(T),[46] in conjunction with the cc-pVTZ[47] basis set and within the frozen-core (fc) approximation, is corrected for the contributions due to the extrapolation to the complete basis set (CBS) limit and to the core-valence (CV) correlation effects, evaluated using second-order Møller-Plesset theory (MP2):[48]

$$E(\text{ChS}) = E(\text{fc-CCSD(T)/cc-pVTZ}) + \Delta E(\text{CBS}) + \Delta E(\text{CV}) \qquad (1)$$

i. $\Delta E(\text{CBS})$ accounts for the extrapolation to the CBS limit; this term is computed by means of the two-point n^{-3} extrapolation formula of ref. 49, with n = 3 (cc-pVTZ), 4 (cc-pVQZ).

ii. $\Delta E(\text{CV})$ recovers the CV contribution. This term is calculated as the difference between all-electrons and fc-MP2 calculations, both with the same cc-pCVTZ basis set.[50]

Electronic energies need to be further corrected for the BSSE error using the CP method, thus leading to the final ChS-CP energies. Zero-point energy (ZPE) corrections have been incorporated within the harmonic approximation at the B2 level (ChS-CP-ZPE).

Analogously, the equilibrium structures of methylamine-water (MAW) and of the two isomers of ethylamine-water complexes (ETW and EGW) have been optimized at the B2 and B2-CP level, and their interaction energy at the B2-CP level.

To spectroscopically characterize all PA-/IPA-W isomers, anharmonic force field calculations have been performed at the B3LYP-D3(BJ)/SNSD level[51,52] (hereafter denoted as B3). Within vibrational perturbation theory to second order[53,54], these allow for the derivation of the vibrational corrections to rotational constants (ΔB^i_{vib}), which have been used to correct the equilibrium rotational constants (B^i_e) straightforwardly derived from the equilibrium structure evaluations:[53]

$$B^i_0 = B^i_e\,(\text{B2-CP}) + \Delta B^i_{vib}(\text{B3}) = B^i_e - \frac{1}{2}\sum_r \alpha^i_r \qquad (2)$$

where the α^i_r's are the vibration-rotation interaction constants, *i* refers to the inertial axes (*a*, *b* and *c*), and the sum runs over the *r* vibrational normal modes. B^i_0's denote the vibrational ground-state rotational constants. At the same time, the B2 harmonic force field provides, as a byproduct, predictions for quartic centrifugal distortion constants.

Because of the presence of a nitrogen atom (nuclear spin I = 1), the corresponding nuclear quadrupole coupling constants represent additional important spectroscopic parameters. To evaluate the corresponding tensor, the components of the electric field gradient tensor at the nitrogen nucleus have been computed at the B2 level. From them, the components of the nitrogen quadrupole coupling constants have then been obtained by means of the following expression:

$$\chi_{ij}(\text{MHz}) = 234.9647 \times Q(\text{barn}) \times q_{ij}(\text{a.u.}) \quad (3)$$

where the first term on the right-hand side is a conversion factor. Q(barn) is the ^{14}N quadrupole moment (20.44(3) barn[55]) and q_{ij}'s (a.u.) are the components of the electric field gradient tensor, with *i*, *j* denoting the inertial axes.

Dipole moment components along the inertial axes, which in turn determine the type and the intensity of transitions observable in the rotational spectra, have been evaluated at the B2 level.

All computations have been performed using the Gaussian 16[56] program package.

Experimental Section

Samples of PA (≥99%) and IPA (≥99%), both purchased from Adamas, were used without any further purification. A gas mixture of 1% PA (or IPA) in helium at a stagnation pressure of 0.2 MPa was streamed over water (main isotopologue, with $H_2{}^{18}O$ and HOD also considered), and supersonically expanded through a solenoid valve (Parker-General Valve, Series 9, nozzle diameter 0.5 mm) into the Fabry-Pérot cavity of the spectrometer.

Rotational spectra of the PA-W and IPA-W adducts were recorded in the 2.0-20.0 GHz frequency range using a highly integrated supersonic-jet Fourier-Transform Microwave (FTMW) spectrometer,[57] with a coaxially oriented beam-resonator arrangement (COBRA-type[58]), which has been described in detail elsewhere.[59] The spectral line positions were determined after Fourier transformation of the time-domain signal with 8k data points, recorded with 100 ns sample intervals. Each transition appears split into a Doppler doublet due to the coaxial resonator arrangement of the supersonic jet, the line position being obtained as the arithmetic mean of the frequencies of the two Doppler components. The estimated accuracy for frequency measurements is better than 3 kHz and the resolution better than 6 kHz.

Figure 1. Stable isomers of the IPA-W and PA-W adducts. The isomers within the frames (green for IPA-W, light blue for PA-W) have been experimentally observed.

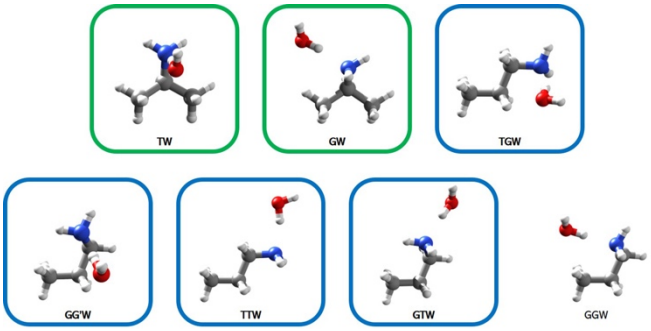

Table 1. Spectroscopic parameters and relative energies of the PA-W and IPA-W adducts.[a]

		PA-W					IPA-W	
		TGW	GG'W	TTW	GTW	GGW	TW	GW
A_0/MHz	theo.	5378.9	4963.8	9895.1	11290.1	4818.3	4805.5	7239.2
	exp.	5466.2596(9)[b]	5003.9028(9)	9977.1499(8)	11477.9594(7)	_	4880.478(2)	7271.1043(1)
B_0/MHz	theo.	2180. 5	2450.3	1452.8	1471.6	2608.0	2520.2	2101.3
	exp.	2172.6407(3)	2411.8257(3)	1467.3249(3)	1478.4918(2)	_	2496.0733(8)	2102.8262(3)
C_0/MHz	theo.	1686.2	1995.4	1307.6	1418.1	1835.9	2425.5	1799.2
	exp.	1688.9887(2)	1979.0333(3)	1319.2830(2)	1427.6159(2)	_	2401.5471(7)	1805.9597(3)
χ_{aa}/MHz	theo.	-0.35	-1.61	-3.27	-4.10	-0.98	-2.88	-3.95
	exp.	-0.400(3)	-1.626(2)	-3.195(5)	-3.963(5)	_	-2.730(3)	-3.825(8)
$(\chi_{bb}-\chi_{cc})$/MHz	theo.	-3.52	-2.74	-0.31	0.60	-3.12	0.75	-0.10
	exp.	-3.232(4)	-2.387(3)	-0.198(6)	0.627(6)	_	0.731(7)	-0.131(9)
ΔE/kJ mol^{-1}		0 (0.16)[c]	0.96 (0.88)	1.59 (0)	2.87 (1.26)	3.92 (1.15)	0 (0)	2.31 (2.02)
ΔE_0/kJ mol^{-1}		0	1.35	0.94	2.45	4.00	0	1.91

[a] Ground-state rotational constants (A_0, B_0, C_0) from B2-CP equilibrium rotational constants augmented by vibrational corrections at the B3LYP-D3(BJ)/SNSD level (for details, see the SI). Nitrogen quadrupole coupling constants (χ_{ii}, with *i*=*a*,*b*,*c*) at the B2 level. Equilibrium (ΔE) and ZPE-corrected (ΔE_0) relative energies at the ChS-CP and ChS-CP-ZPE level, respectively. [b] Standard errors within parentheses are expressed in units of the last digit. [c] Values in parentheses are the relative energies of the isolated amine conformers at the ChS level.

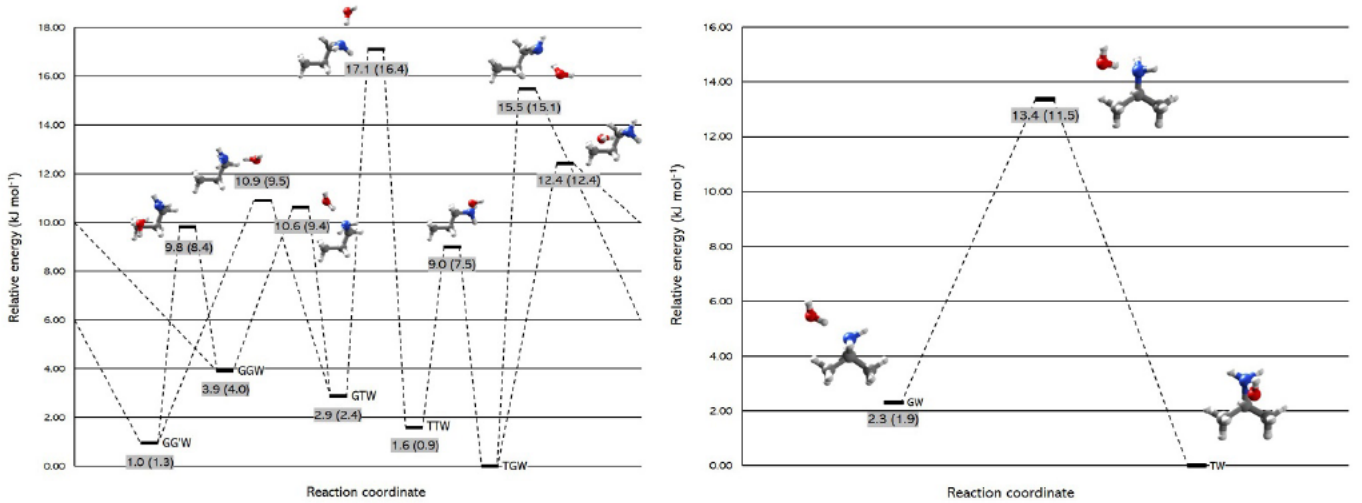

Figure 2. Isomerization profile for the PA-W (left panel) and IPA-W (right panel) adducts: ChS-CP and ChS-CP-ZPE (within parentheses) relative energies in kJ mol^{-1}.

Results and Discussion

All possible isomers of the PA/IPA-W systems obtained from the computational search are depicted in Figure 1. Two stable isomers have been identified for the IPA-W adduct, where IPA adopts *trans* (TW) or *gauche* (GW) conformation. As far as PA-W is concerned, five stable isomers have been located on the PES, which are labelled as TGW, GG'W, TTW, GTW and GGW, where the first two letters denote the PA conformer involved in the molecular complex with water. The notation used for the PA conformers is based on the τ(CCCN) dihedral angle of the skeletal frame and the orientation of the lone pair in amino group (τ(CCN-lp)). The relative stability of the minima together with that of the transition states ruling their interconversion are shown in Figure 2 (left panel for PA-W, right panel for IPA-W). As already noted for n-propanol,[60-62] the water cluster formation modifies the relative stability of the different isomers with respect to the corresponding isolated amine. In the case of PA, the complexation with water leads –in relative terms– to a destabilization of the TT, GT and GG conformers and to a stabilization of TG and GG' (see Table 1).

Computed spectroscopic parameters and relative energies of all PA-/IPA-W isomers are collected in Table 1, with a more extended version of this table reported in the Supporting Information (SI). Spectral searches using simulations based on the spectroscopic parameters reported in Table 1 have been performed following the stability order. For PA-W, TGW was firstly observed and assigned. After its frequencies were removed from the spectrum, rotational transitions of the GG'W, TTW and GTW isomers have been then easily assigned thanks to their characteristic ^{14}N quadrupole hyperfine patterns (see Figure 3). In agreement with its relative stability (and thus its low population), no lines belonging to GGW have been found. The experimental outcomes are in line with the computed stabilities and the barrier heights ruling the interconversion (Figure 2). For the IPA-W adduct, the assignment of the rotational spectra of both isomers was straightforward thanks again to the characteristic hyperfine structure due to the nitrogen quadrupole coupling (see Figure 3).

For all molecular complexes, the measured transition frequencies have been fitted, using Pickett's SPFIT program,[63] to Watson's semirigid-rotor Hamiltonian[64] (I^r representation, *S*-reduction). Selected spectroscopic parameters are listed in Table 1 for the main isotopic species, while all measured transition frequencies as well as the complete list of the spectroscopic constants are available in the SI. In all cases, the standard deviation of the fit is small and on the order of the measurement accuracy (i.e. 2-4 kHz). In addition to the main isotopic species, water isotopologues were also investigated. As far as the PA-W isomers are concerned, the rotational spectra of the molecular complexes with ^{18}O-enriched water and DOH (with D involved in the HB) have been assigned. For the IPA-W isomers, transitions belonging to the IPA-$H_2{}^{18}O$/DOH/HOD isotopologoues could be successfully identified. The spectroscopic parameters for all isotopic species are summarized in the SI.

The comparison between experimental and computed spectroscopic parameters points out an overall good agreement. For rotational constants, the differences –in relative terms– range between 0.1% and 1.6%, which can be considered a very good result in view of the high flexibility of the systems under consideration. Analogously, the nuclear quadrupole coupling constants are well predicted. The good agreement noted for these two sets of spectroscopic parameters, which are strongly related to the molecular structure, suggests that the B2(-CP) level is suitable for describing flexible intermolecular complexes.

For each isomer observed, the investigation of different isotopologues has opened the way to the determination of a partial semi-experimental (SE) equilibrium structure (r_e^{SE}). This approach is based on a least-squares fit of the experimental ground-state rotational constants computationally corrected for vibrational contributions.[10]

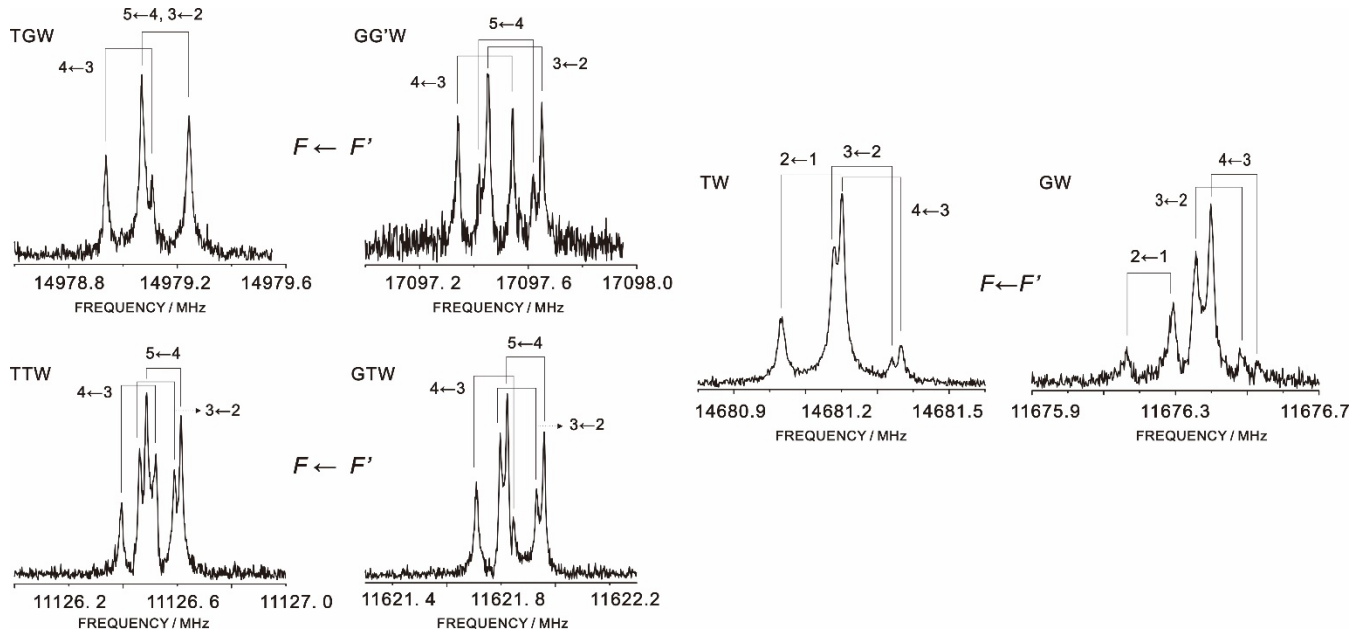

Figure 3. Left panel: the $4_{0,4}$←$3_{0,3}$ rotational transition for the TGW, GG'W, TTW and GTW isomers. Right panel: the $3_{0,3}$←$2_{0,2}$ rotational transition of the TW and GW isomers. All spectra show the characteristic hyperfine structure and Doppler doubling. Hyperfine components are labelled using the *F* quantum number coming from the *F* = *I* + *J* coupling scheme, with I being the nuclear spin of ^{14}N and J the rotational quantum number.

As shown in eq. (2), equilibrium rotational constants B_e^i's differ from the vibrational ground-state ones B_0^i's –derived from the spectral analysis– for a contribution that can be reliably computed ($\Delta B_{vib}^i = -1/2 \sum_r \alpha_r^i$).[11,65] The resulting equilibrium rotational constants are thus defined as semi-experimental because of the mixed contributions. Although the number of isotopologues investigated in the present work is not sufficient for a complete structural characterization, they anyway allow the determination of the intermolecular parameters with an experimental-quality accuracy.[11,65,66]

The intramolecular bond lengths and angles have been kept fixed at their scaled values, which were obtained by means of the template approach.[11] While we refer the reader to ref. 11 for a detailed account, in the following the key aspects of this methodology are summarized. The structural parameters that cannot be determined in the fit are corrected by using high-level calculations performed for a smaller system, referred to as templating model (TM), which contains a similar structural frame:

$$r_e = r_e^{\mathrm{B2}} + \Delta\mathrm{TM} \ . \qquad (4)$$

r_e^{B2} is the geometrical parameter obtained at the B2 level for the system under investigation, while ΔTM is the difference between the B2 equilibrium parameter and the corresponding reference value (in the present case, at the ChS+AUG level) for the TM molecule:

$$\Delta\mathrm{TM} = r_e^{\mathrm{ChS+AUG}}(\mathrm{TM}) - r_e^{\mathrm{B2}}(\mathrm{TM}) \ . \qquad (5)$$

"ChS+AUG" denotes the ChS approach for geometries, which is analogous to the ChS model for energies, but it also includes a contribution for incorporating the effects of diffuse functions in the basis set ($\Delta r(\mathrm{aug})$):[43]

$$r(\mathrm{ChS+AUG}) = r(\mathrm{CC/VTZ}) + \Delta r(\mathrm{CBS}) + \Delta r(\mathrm{core}) + \Delta r(\mathrm{aug}) \quad (6)$$

where $\Delta r(\mathrm{aug})$ is calculated as the difference between MP2 calculations with the aug-cc-pVTZ[67] and cc-pVTZ basis sets, within the frozen-core approximation.

In eqs. (4) and (5), TMs are the two monomers, the PA or IPA isolated isomer and the water molecule. The MSR software[68] has been used for the structural determinations above, with all rotational constants being equally weighted.

The SE intermolecular parameters obtained from the fit are collected in Table 2 and compared with their QC counterparts. It is noted that the two sets of values are in a reasonably good agreement, with the largest discrepancies noted for the ∠HON angle (with H being the hydrogen atom involved in the HB), which is –however– the worse determined parameter. It is noteworthy that exclusion of the ∠HON angle from the fit affects only negligibly the final values of the other two parameters.

Comparison of the computed intermolecular parameters of the PA- and IPA-W isomers with those of MAW, ETW and EGW shows that the O···N intermolecular distance remains nearly unchanged along the series, this ranging from 2.87 Å to 2.89 Å at the B2 level and from 2.89 Å to 2.90 Å at the B2-CP level. This comparison suggests that the length of the alkyl chain and also its ramification do not have a relevant effect on the intermolecular interactions.

To shed light on the intermolecular interactions taking place in the molecular complexes investigated, different analyses have been carried out. The first one considered is the Johnson's non-covalent interaction (NCI) analysis,[69,70] which has been performed using the Multiwfn program.[71] The results are graphically shown in Figure 4, where the iso-surfaces of the reduced density gradient are shown together with a color legend box for the interaction strength. It is first of all noted that all molecular complexes present one strong O-H···N HB as primary interaction, which is –in the case of the TGW, GGW and GW isomers– associated with one weaker C-H···O HB.

Table 2. SE[a] (first row) and B2-CP (second row; B2 given in parentheses underneath) intermolecular parameters in the alkyl amine-water complexes.

	MAW	ETW	EGW	TW	GW	TGW	GG'W	TTW	GTW
$R_{O\cdots N}$/Å	2.890 (2.877)	2.893 (2 879)	2.890 (2.876)	2.9135(4) 2.903 (2.889)	2.894(1) 2.887 (2.872)	2.88134(3) 2.888 (2.873)	2.895(1) 2.897 (2.882)	2.88586(6) 2.893 (2.879)	2.8830(6) 2.892 (2.879)
∠ONC/°	96.06 (95.76)	96.69 (96.37)	97.96 (97.33)	102.35(2) 101.29 (100.75)	98.61(6) 98.66 (98.05)	97 9754(2) 97.58 (96.95)	101.34(3) 102.06 (100.40)	96 6001(8) 96 90 (96.53)	97.44(4) 96.69 (96.29)
∠HON[b]/°	9.22 (9.33)	8.96 (9.08)	9.31 (9.61)	3.08(28) 8.54 (8.74)	5.78(83) 9.18 (9.47)	7.63(2) 9.42 (9.74)	4.48(93) 7.87 (8.33)	8.06(6) 8.80 (8.91)	7.39(13) 8.76 (8.88)
∠OHN[b]/°	166.14 (165.94)	166.52 (166.31)	166.00 (165.51)	175.36[c] 167.17 (166.83)	171.30[c] 166.17 (165.70)	168.50[c] 165.82 (165.30)	173.24[c] 168.16 (167.44)	167.86[c] 166.77 (166.56)	168.86[c] 166.82 (166.61)

[a] The uncertainty reported is one standard deviation of the fit. [b] The H atom is the one involved in the HB. [c] Derived parameter.

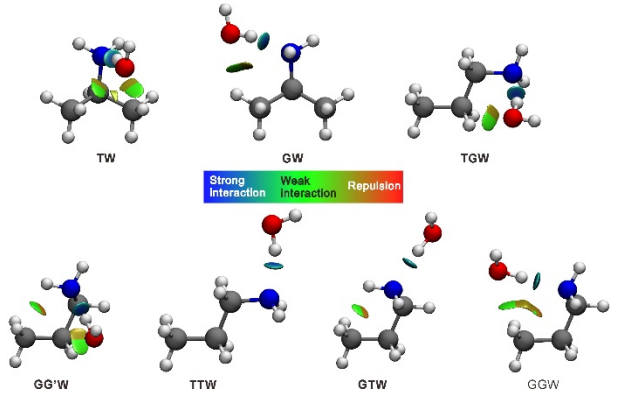

Figure 4. Color-filled (color scale given in the inset) NCI isosurfaces of the reduced electron density gradient (*s* = 0.5). Isomers in bold have been experimentally observed.

For the TW isomer, two weak C-H···O HBs are present together with the primary interaction, while in the case of the TTW isomer no additional interactions are found. The GTW conformer shows, instead of an additional intermolecular HB, a weak intramolecular N-H···C interaction. Finally, the terminal methyl group of the GG'W conformer is able to form both intramolecular (N-H···C) and intermolecular (C-H···O) weak HBs.

To go deeper into the analysis of non-covalent interactions and to unravel their nature, the Symmetry-Adapted Perturbation theory (SAPT)[72,73] EDA has been carried out at the SAPT2+3(CCD)/aug-cc-pVDZ-RI level using the PSI4 program.[74] The results are sketched in Figure 5 and tabulated in the SI (Table S25), where the values for the water dimer as well as for MAW, ETW and EGW have been reported for comparison purposes. Focusing on PA-/IPA-W complexes, the interaction energies range between 29 and 32 kJ mol^{-1} for all isomers (between 31.2 and 33.5 kJ mol^{-1} and between 31.5 and 34.1 kJ mol^{-1} at the B2-CP and ChS level, respectively; see Table S25) and also the individual contributions are similar. Inspection of the various contributions (see Table S25 and Figure 5) makes it clear that the largest contribution is the repulsive exchange term, which is nearly compensated by the electrostatic contribution. The induction and dispersion terms, which are rather similar to one another, amount together to about two-thirds of the electrostatic contribution. For MAW as well as ETW and EGW, the situation is very similar both in terms of the single contributions and the overall interaction energy (ranging from ~29 to 31 kJ mol^{-1}). It is interesting to note that the interaction energies of all these complexes are about 50% larger than that of the water dimer, thus indicating that the primary interaction (O-H···N) occurring in the alkyl amine-water complexes is stronger than the O-H···O HB in the water dimer, as expected in view of the greater basicity of amines with respect to water. Overall, the data suggest that the lengthening of the alkyl chain and its ramification have a limited influence on the intermolecular interaction, its strength only marginally increasing along the series. This outcome confirms the overall conclusion drawn from the analysis of the intermolecular parameters.

The SAPT results point out that the interaction between PA and water is stronger in the case of the TG and GG' conformers with respect to TT, GT and GG by about 2 kJ mol^{-1}. On the contrary, the strength of the interaction is nearly the same for the two IPA conformers. This explains the above-mentioned change of the stability order for the PA conformers when going from the isolate amine to the corresponding water complex, and also why the relative stability remains unchanged for the two IPA conformers.

The results of the natural bond order (NBO) analysis[75] (performed at the B3LYP-D3(BJ)/maug-cc-pVTZ-*d*H level of theory and detailed in the SI) point out that the strength of the O-H···N HB, i.e. the interaction between the nitrogen lone pair and the antibonding O-H orbital, is very similar for all the complexes, with the second-order perturbation contribution to the complex stabilization ranging between 12.5 and 13.5 kJ mol^{-1}. This contribution is accompanied, except for TTW and GTW, by weaker interactions between the oxygen lone-pair(s) and CH antibonding orbital(s).

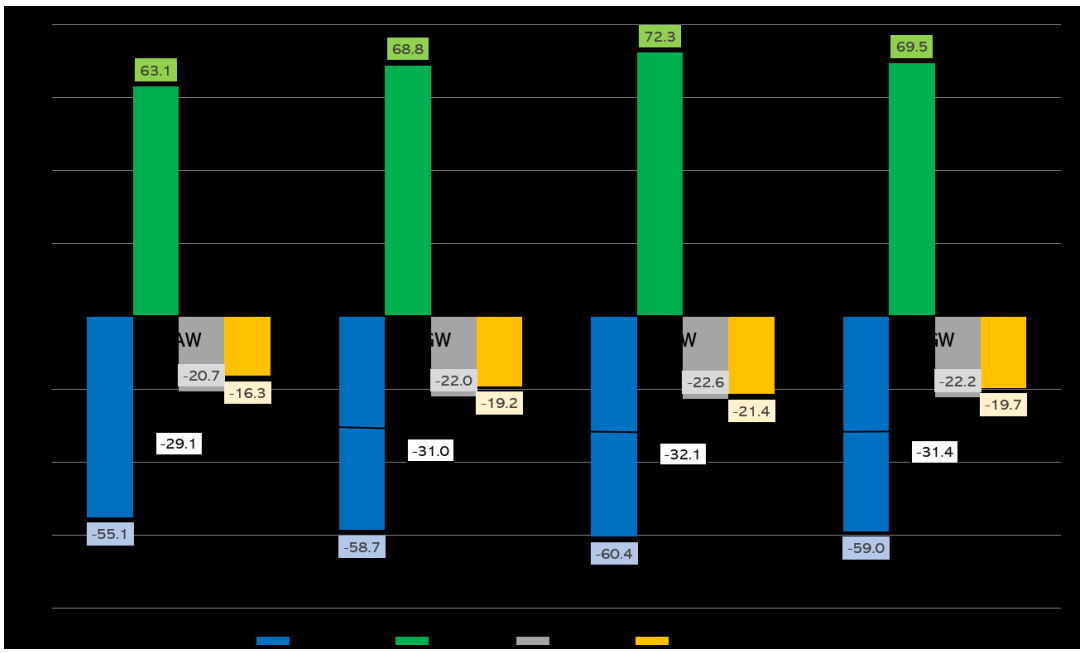

Figure 5. Summary of the SAPT energy contributions (in kJ mol^{-1}) for the methylamine-water (MAW), ethylamine-water (EGW), iso-propylamine-water (TW), and n-propylamine-water (TGW) complexes. When applies, the most stable isomer is considered.

Finally, starting from the interaction energy (E_{int}), the inclusion of the deformation contribution (Δ_{def}) leads to the evaluation of the dissociation energy ($D_e = E_{int} - \Delta_{def}$; see e.g. ref. 76). For the most stable isomers, i.e. TGW and TW, the Δ_{def} is -1.48 and -1.56 kJ mol^{-1}, respectively. Using the data reported in Table S25, this results in D_e being -32.03 and -32.56 kJ mol^{-1} for TGW and TW, respectively.

Conclusions

In the present work, state-of-the-art quantum-chemical methodologies have been combined with rotational spectroscopy in supersonic expansion to unveil the intermolecular interactions established in alkyl amines-water complexes. While the joint experimental-computational approach has been applied to the characterization of the PA-W and IPA-W adducts, the theoretical investigation has been extended to smaller amines, here considering the complexes formed by methylamine and ethylamine (both *gauche* and *trans* conformers) with water. The comparison of the intermolecular parameters and interaction energies pointed out that the length of the alkyl chain has a very limited effect. This result thus suggests the transferability of the outcomes of the present work to larger alkyl amines, possibly of biological interest.

For all the PA-/IPA-W isomers experimentally observed, the recording and assignment of the rotational spectra of different isotopic species allowed the semi-experimental determination of the intermolecular parameters, which also pointed out the reliability and accuracy of B2(-CP) calculations for structural investigations. Therefore, this work proves that state-of-the-art QC methods coupled to rotational spectroscopy experiments can be confidently employed to obtain equilibrium structures of unprecedented accuracy for non-covalent complexes in the gas phase.

Different energy decomposition analyses, namely NBO and SAPT, agreed in pointing out that the primary interaction is a strong O-H···N HB: the repulsive exchange contribution is nearly compensated by the electrostatic term, while those due to induction and dispersion amount together to two-thirds of the latter contribution, thus leading to an overall interaction energy ranging from ~29 to 32 kJ mol^{-1}. This picture has been complemented by the NCI analysis, which allowed for better visualizing the number of non-covalent interactions occurring and their strength.

In summary, together with the remarkable intrinsic interest of the studied systems, this work confirms the effectiveness and reliability of combined quantum chemistry – rotational spectroscopy investigations to unveil the role of different physical-chemical factors in tuning the structural and energetic features of non-covalent molecular complexes.

Conflicts of interest

There are no conflicts to declare.

Acknowledgements

Support from the Italian MIUR (PRIN 2015, Grant Number 2015F59J3R; PRIN 2017, Grant Number 2017A4XRCA) is acknowledged. This work has also been supported by the University of Bologna (RFO funds). We are grateful for support from: National Natural Science Foundation of China (21703021 and U1931104); Fundamental and Frontier Research Fund of Chongqing (cstc2017jcyjAX0068 and cstc2018jcyjAX0050);

Venture & Innovation Support Program for Chongqing Overseas Returns (cx2018064); Foundation of 100 Young Chongqing University (0220001104428); Fundamental Research Funds for the Central Universities (2018CDQYHG0009). The authors also thank Dr. Silvia Alessandrini for useful discussions.

Notes and references

1 C. Pérez, J. L. Neill, M. T. Muckle, D. P. Zaleski, I. Peña, J. C. Lopez, J. L. Alonso, B. H. Pate, *Angew. Chem. Int. Ed.* 2015, **54**, 979-982.

2 C. Pérez, D. P. Zaleski, N. A. Seifert, B. Temelso, G. C. Shields, Z. Kisiel, B. H. Pate, *Angew. Chem. Int. Ed.* 2014, **53**, 14368-14372.

3 J. Wang, L. Spada, J. Chen, S. Gao, S. Alessandrini, G. Feng, C. Puzzarini, Q. Gou, J.-U. Grabow, V. Barone, *Angew. Chem. Int. Ed.* 2019, **58**, 13935-13941.

4 D. A. Obenchain, L. Spada, S. Alessandrini, S. Rampino, S. Herbers, N. Tasinato, M. Mendolicchio, P. Kraus, J. Gauss, C. Puzzarini, J.-U. Grabow, V. Barone, *Angew. Chem. Int. Ed.* 2018, **57**, 15822-15826.

5 N. W. Ulrich, T. S. Songer, R. A. Peebles, S. A. Peebles, N. A. Seifert, C. Pérez, B. H. Pate, *Phys. Chem. Chem. Phys.* 2013, **15**, 18148-18154.

6 J. C. López, R. Sánchez, S. Blanco, J. L. Alonso, *Phys. Chem. Chem. Phys.* 2015, **17**, 2054-2066.

7 C. Calabrese, W. Li, G. Prampolini, L. Evangelisti, I. Uriarte, I. Cacelli, S. Melandri, E. J. Cocinero, *Angew. Chem. Int. Ed.* 2019, **58**, 8437-8442.

8 W. Li, L. Evangelisti, Q. Gou, W. Caminati, R. Meyer, *Angew. Chem. Int. Ed.* 2019, **58**, 859-865.

9 G. Karir, N. O. B. Lgttschwager, M. A. Suhm, *Phys. Chem. Chem. Phys.* 2019, **21**, 7831-7837.

10 P. Pulay, W. Meyer, J. E. Boggs, *J. Chem. Phys.* 1978, **68**, 5077-5085.

11 M. Piccardo, E. Penocchio, C. Puzzarini, M. Biczysko, V. Barone, *J. Phys. Chem. A* 2015, **119**, 2058-2082.

12 V. Barone, M. Biczysko, J. Bloino, P. Cimino, E. Penocchio, C. Puzzarini, *J. Chem. Theory Comput.* 2015**, 11**, 4342-4363.

13 M. C. McCarthy, L. Cheng, K. N. Crabtree, O. Martinez, T. L. Nguyen, C. C. Womack, J. F. Stanton, *J. Phys. Chem. Lett.* 2013, **4**, 4133-4139.

14 O. Martinez, K. N. Crabtree, C. A. Gottlieb, J. F. Stanton, M. C. McCarthy, *Angew. Chem. Int. Ed.* 2015, **54**, 1808-1811.

15 U. Spoerel, W. Stahl, *J. Mol. Spectrosc.* 1998, **190**, 278-289.

16 S. Melandri, A. Maris, B. M. Giuliano, L. B. Favero, W. Caminati, *Phys. Chem. Chem. Phys.* 2010, **12**, 10210-10214

17 I. Yoon, K. Seo, S. Lee, Y. Lee, B. Kim, *J. Phys. Chem. A* 2007, **111**, 1800-1807.

18 R. Brause, H. Fricke, M. Gerhards, R. Weinkauf, K. Kleinermanns, *Chem. Phys.* 2006, **327**, 43-53.

19 N. Mayorkas, S. Cohen, H. Sachs, I. Bar, *RSC Adv.* 2014, **4**, 58752- 58757.

20 E. G. Robertson, J. P. Simons, *Phys. Chem. Chem. Phys.* 2001, **3**, 1-18.

21 R. D. Hoehn, M. A. Carignano, S. Kais, C. Zhu, J. Zhong, X. C. Zeng, J. S. Francisco, I. Gladich, *J. Chem. Phys.* 2016, **144**, 214701.

22 P. J. Silva, M. E. Erupe, D. Price, J. Elias, Q. G. J. Malloy, Q. Li, B. Warren, D. R. Cocker, *Environ. Sci. Technol.* 2008, **42**, 4689-4696.

23 J.-S. Youn, E. Crosbie, L. C. Maudlin, Z. Wang, A. Sorooshian, *Atmos. Environ.* 2015, **122**, 250-258.

24 A. Lavi, N. Bluvshtein, E. Segre, L. Segev, M. Flores, Y. Rudich, *J. Phys. Chem. C* 2013, **117**, 22412-22421.

25 C. Qiu, R. Zhang, *Phys. Chem. Chem. Phys.* 2013, **15**, 5738-5752.

26 G. A. Jeffray, T. H. Jordan, R. K. Mullan, *Science* 1967, **155**, 689-691.

27 F. H. Herbstein, in *Crystalline Molecular Complexes and Compounds, Structures and Principles, Vol. 1*, IUCr Monographs on Crystallography 18, Oxford University Press, 2005, p. 389.

28 O. Mousis, J. I. Lunine, S. Picaud, D. Cordier, *Faraday Discuss.* 2010, **147**, 509-525.

29 K.E. Mandt, O. Mousis, B. Marty, T. Cavalié, W. Harris, P. Hartogh, K. Willacy, *Space Sci. Rev.* 2015, **197**, 297-342.

30 *Nanoscience and Nanoengineering: Advances and Applications*, ed. A. D. Kelkar, D. J.C. Herr and J. G. Ryan, CRC Press, 2014.

31 B. H. Atak, B. Buyuk, M. Huysal, S. Isik, M. Senel, W. Metzger, G. Cetin, *Carbohydr. Polym.* 2017, **164**, 200-213.

32 W. L. Jorgensen, J. Tirado-Rives, *Proc. Nat. Acad. Sci.* 2005, **102**, 6665-6670.

33 M. M. Lencka, J. J. Kosinski, P. Wang, A. Anderko, *Fluid Phase Equilibria* 2016, **418**, 160-174.

34 W. Li, L. Spada, N. Tasinato, S. Rampino, L. Evangelisti, A. Gualandi, P. G. Cozzi, S. Melandri, V. Barone, C. Puzzarini, *Angew. Chem. Int. Ed.* 2018, **57**, 13853-13857.

35 S. Grimme, *J. Chem. Phys.* 2006, **124**, 034108.

36 S. Grimme, J. Anthony, S. Ehrlich, H. Krieg, *J. Chem. Phys.* 2010, **132**, 154104.

37 S. Grimme, S. Ehrlich, L. Goerigk, *J. Comput. Chem.* 2011, **32**, 1456-1465.

38 E. Papajak, H. R. Leverentz, J. Zheng, D. G. Truhlar, *J. Chem. Theory Comput.* 2009, **5**, 1197-1202.

39 T. Fornaro, M. Biczysko, J. Bloino, V. Barone, *Phys. Chem. Chem. Phys.* 2016, **18**, 8479- 8490.

40 S. F. Boys, F. Bernardi, *Mol. Phys.* 1970, **19**, 553-566.

41 P. Salvador, B. Paizs, M. Duran, S. Suhai, *J. Comput. Chem.* 2001, **22**, 765-786.

42 M. Biczysko, G. Scalmani, J. Bloino, V. Barone, *J. Chem. Theory Comput.* 2010, **6**, 2115-2125.

43 C. Puzzarini, V. Barone, *Phys. Chem. Chem. Phys.* 2011, **13**, 7158-7166.

44 C. Puzzarini, M. Biczysko, V. Barone, I. Peña, C. Cabezas, J. L. Alonso, *Phys. Chem. Chem. Phys.* 2013, **15**, 16965-16975.

45 C. Puzzarini, M. Biczysko, *J. Phys. Chem. A* 2015, **119**, 5386-5395.

46 a) K. Raghavachari, G. W. Trucks, J. A. Pople, *Chem. Phys. Lett.* 1989, **157**, 479-483. b) G. D. Purvis III, R. J. Bartlett, *J. Chem. Phys*. 1982, **76**, 1910-1918.

47 T.H. Dunning Jr., *J. Chem. Phys*. 1989, **90**, 1007-1023.

48 C. Møller, M. S. Plesset, *Phys. Rev*. 1934, **46**, 618-622.

49 T. Helgaker, W. Klopper, H. Koch, J. Noga, *J. Chem. Phys*. 1997, **106**, 9639-9646.

50 D. E. Woon, T. H. Dunning, *J. Chem. Phys.* 1995, **103**, 4572-4585.

51 a) D. Becke, *J. Chem. Phys*. 1993, **98**, 5648-5652. b) J. P. Perdew, K. Burke, Y. Wang, *Phys. Rev. B* 1996, **54**, 16533-16539.

52 Double and Triple-Zeta basis sets of the SNS family, are available in the Download section: http://smart.sns.it/

53 I. M. Mills in *Molecular Spectroscopy*: Modern Research, ed. K.N. Rao and C.W. Mathews, Academic Press, 1972.
54 V. Barone, J. Chem. Phys. 2005, **122**, 014108.
55 P. Pyykkö, *Mol. Phys.* 2008, **106**, 1965-1974.
56 *Gaussian 16*, Revision B.01, M. J. Frisch, G. W. Trucks, H. B. Schlegel, G. E. Scuseria, M. A. Robb, J. R. Cheeseman, G. Scalmani, V. Barone, G. A. Petersson, H. Nakatsuji, X. Li, M. Caricato, A. V. Marenich, J. Bloino, B. G. Janesko, R. Gomperts, B. Mennucci, H. P. Hratchian, J. V. Ortiz, A. F. Izmaylov, J. L. Sonnenberg, D. Williams-Young, F. Ding, F. Lipparini, F. Egidi, J. Goings, B. Peng, A. Petrone, T. Henderson, D. Ranasinghe, V. G. Zakrzewski, J. Gao, N. Rega, G. Zheng, W. Liang, M. Hada, M. Ehara, K. Toyota, R. Fukuda, J. Hasegawa, M. Ishida, T. Nakajima, Y. Honda, O. Kitao, H. Nakai, T. Vreven, K. Throssell, J. A. Montgomery, Jr., J. E. Peralta, F. Ogliaro, M. J. Bearpark, J. J. Heyd, E. N. Brothers, K. N. Kudin, V. N. Staroverov, T. A. Keith, R. Kobayashi, J. Normand, K. Raghavachari, A. P. Rendell, J. C. Burant, S. S. Iyengar, J. Tomasi, M. Cossi, J. M. Millam, M. Klene, C. Adamo, R. Cammi, J. W. Ochterski, R. L. Martin, K. Morokuma, O. Farkas, J. B. Foresman, and D. J. Fox, Gaussian, Inc., Wallingford CT, 2016.
57 T. J. Balle., W. H. Flygare, *Rev. Sci. Instrum.* 1981, **52**, 33-45.
58 J.-U. Grabow, W. Stahl, H. Dreizler, *Rev. Sci. Instrum.* 1996, **67**, 4072-4084.
59 J.-U. Grabow, Q. Gou, G. Feng, in *72nd International Symposium on Molecular Spectroscopy*, TH03, Champaign-Urbana, 2017.
60 T. N. Wassermann, P. Zielke, J. J. Lee, C. Cézard, M. A. Suhm, *J. Phys. Chem. A* 2007, **111**, 7437-7448.
61 Z. Kisiel, O. Dorosh, A. Maeda, I. R. Medvedev, F. C. De Lucia, E. Herbst, B. J. Drouin, J. C. Pearson, *Phys. Chem. Chem. Phys.* 2010, **12**, 8329-8339.
62 G. J. Mead, E. R. Alonso, I. A. Finneran, P. B. Carroll, G. A. Blake, *J. Mol. Spectrosc.* 2017, **335**, 68-73.
63 H. M. Pickett, *J. Mol. Spectrosc.* 1991, **148**, 371-377.
64 J. K. G. Watson, in *Vibrational Spectra and Structure*, ed. J.R. Durig, Elsevier, 1977, p. 1.
65 F. Pawlowski, P. Jørgensen, J. Olsen, F. Hegelund, T. Helgaker, J. Gauss, K. L. Bak, J. F. Stanton, *J. Chem. Phys.* 2002, **116**, 6482-6496.
66 C. Puzzarini, V. Barone, *Acc. Chem. Res.* 2018, **51**, 548-556.
67 R. A. Kendall, T. H. Dunning, Jr., R. J. Harrison, *J. Chem. Phys*. 1992, **96**, 6796.
68 M. Mendolicchio, E. Penocchio, D. Licari, N. Tasinato, V. Barone, *J. Chem. Theory Comput.* 2017, **13**, 3060-3075.
69 E. R. Johnson, S. Keinan, P. Mori-Sanchez, J. Contreras-Garcia, A. J. Cohen, W. Yang, *J. Am. Chem. Soc.* 2010, **132**, 6498-6506.
70 R. F. W. Bader, *Chem. Rev.* 1991, **91**, 893-928.
71 T. Lu, F. Chen, *J. Comput. Chem.* 2012, **33**, 580-592.
72 B. Jeziorski, R. Moszynski, K. Szalewicz, *Chem. Rev.* 1994, **94**, 1887-1930.
73 T. M. Parker, L. A. Burns, R. M. Parrish, A. G. Ryno, C. D. Sherrill, *J. Chem. Phys.* 2014, **140**, 094106.
74 R. M. Parrish, L. A. Burns, D. G. A. Smith, A. C. Simmonett, A. E. DePrince III, E. G. Hohenstein, U. Bozkaya, A. Yu. Sokolov, R. Di Remigio, R. M. Richard, J. F. Gonthier, A. M. James, H. R. McAlexander, A. Kumar, M. Saitow, X. Wang, B. P. Pritchard, P. Verma, H. F. Schaefer III, K. Patkowski, R. A. King, E. F. Valeev, F. A. Evangelista, J. M. Turney, T. D. Crawford, and C. D. Sherrill, *J. Chem. Theory Comput.* 2017, **13**, 3185-3197.
75 E. D. Glendening, C. R. Landis, F. Weinhold, *WIREs Comput. Mol. Sci.* 2012, **2**, 1-42.
76 S. Alessandrini, V. Barone, C. Puzzarini, J. Chem. Theory Comput. 2020, **DOI: 10.1021/acs.jctc.9b01037**.